

Research Article

# Transmutation of Elements in Low-energy Glow Discharge and the Associated Processes

I.B. Savvatimova \*

*Podolsk, Moscow Region, Russia*

---

## Abstract

The review of the main transmutation results in palladium and tungsten after the exposure to deuterium Glow Discharge (GD) measured by different Mass Spectrometry (MS) and Gamma-Spectrometry (GS) methods is given. The registered structure and isotopic ratio change alongside with formation of additional elements were accompanied by gamma and X-ray emission. The registered isotopic ratio change ranged within 2–1000 times, the quantity of additional elements undetected before varying within one tenth to dozens percents in Pd and Pd alloys. The isotopes with masses less than and exceeding those of the cathode material were measured in most of the experiments. The MS revealed that the tungsten isotopes transmuted into elements lighter than tungsten, higher post-experimental intensity of mass numbers 169, 170, 171, 178 and 180 being observed. The mass spectra peaks magnituded for isotopes lighter than W isotopes increased by factors ranging from 5 to 400. The registered increase varied from 5–50 cps in the original foils to 100–20 000 cps after the exposure to deuterium GD. Lighter isotopes in tungsten and tantalum foils placed on the GD cathode after deuterium GD exposure were identified using high resolution gamma/X-ray spectrometry. The comparison of thermal ionization mass-spectrometry (TIMS) data and data of gamma-spectra energy peaks allowed to assume that the peaks series observed in gamma spectra belong to the following isotopes:  $^{169}_{70}\text{Yb}$ ,  $^{170}_{72}\text{Hf}$ ,  $^{171m}_{70}\text{Yb}$ ,  $^{172}_{72}\text{Hf}$  and  $^{178}_{70}\text{Yb}$ . Correlation of TIMS and Gamma spectrometry data leads to the assumption that the appearance of light isotopes in tungsten resulted from the low-energy decay process initiation caused by deuterium GD.

© 2012 ISCMNS. All rights reserved.

**Keywords:** Isotopic ratio change, Low-energy gas glow discharge, Mass-spectrometry, Palladium, Transmutation, Tungsten

---

## 1. Introduction

The review of numerous GD experimentation results during and after the irradiation by GD ions starting 1989 and up to the present time is given. The analysis of structure, elemental and isotopic ratio change in the materials exposed to low-energy ions irradiation upon the GD cathode is carried out. Changes in elemental composition, quantity and places of concentration of the newly formed impurity elements depends upon the GD parameters, type of ions (H, D, and Ar), kind of current (direct or pulsed) and the presence of impurities in the cathode. The gamma emission intensity

---

\*E-mail: isavvatim@mail.ru

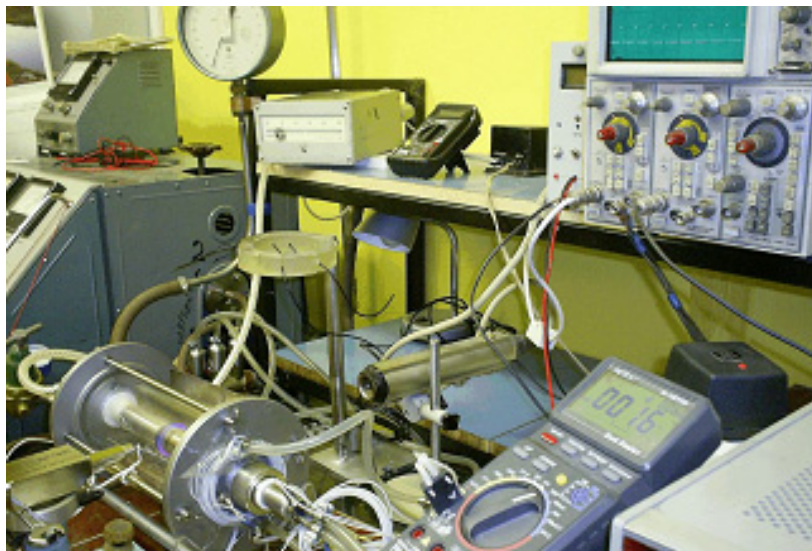


**Figure 1.** The gas glow discharge setup with CdTe detector location: 1- CdTe gamma and X-ray detector.

registration was carried out during the GD ions exposure and after GD current switch off outside the GD chamber. Post-experimental direct measurements of the emission from the cathode material in contact with a gamma-detector were made. Post-experimental changes in an alpha-, beta-, and gamma-intensity in the cathode materials uranium exposed to hydrogen and deuterium ions bombardment, and also the change in the isotopic content and elements composition were observed. The results obtained show that the GD ions low-energy influence stimulates the registered nuclear processes.

In our previous papers [1,2,8], we described elemental and isotopic change in palladium and titanium. Weak gamma-emission, brief neutron bursts [5–7,9], changes of surface structure and of the elemental and isotopic composition in the Pd cathode were observed. The increase in Pd impurities (undetected in the original material) ranged 0.5–5% (an increase by 100–10 000 times).

Post-experimental local blackening of X-ray films placed in contact with Pd, Ti and Ag foils was observed [3,7,8]. Local blackening was also observed [3,9] in X-ray films placed both inside and outside of the GD chamber stainless steel wall. Results of Pd foils radiographic analysis showed presence of high-energy and low-energy components [6] in the films contacting the foils after the exposure. The observed effects are explained by the fusion–fission reaction on the cathode materials (mostly foils), by the interaction between the Pd lattice and Deuterium and by the subsequent decay into lighter elements. The majority of the post-experimental impurities were found in certain local zones (“hot spots”) [1–3,8]. Post-experimental impurity elements (with various content) such as Sc, Ti, V, Ag, Cd, In, P, Cl, Br, Ge, As, Kr, Sr, Y, Ru, and Xe were discovered in the Pd material after the exposure to all types of ions (D, H, Ar, and Ar + Xe). The estimated correlation of the integral sum of all impurity elements in Pd samples after the bombardment by D, H, and Ar ions showed 10:(2 or 3):1, respectively [9]. Considerable change in the isotopic ratios in Pd foils for  $^{10}\text{B}/^{11}\text{B}$ ;  $^{12}\text{C}/^{13}\text{C}$ ;  $^{60}\text{Ni}/^{61}\text{Ni}/^{62}\text{Ni}$ ;  $^{40}\text{Ca}/^{44}\text{Ca}$ , and  $^{90}\text{Zr}/^{91}\text{Zr}$  was registered by different mass-spectrometry methods [6]. Changes in the isotopic ratios for  $^{109}\text{Ag}/^{107}\text{Ag}$  ranged from the initial Pd ratio of 1/1 to 3/1 and 9/1 after the GD exposure (described in [5,9]).

Weak gamma-emissions, short-term neutron bursts, neutron and gamma energy-spectra were registered. This data

**Table 1.** Changes in the isotopic shift and elemental composition of the impurity atoms upon Pd surface after the exposure to D ions bombarding (SIMS) [6].

No.	Mass	Element	Content (arb. units)				
			Before experiment	After experiment			
				Exposed side	Unexposed side	Increase factor	
						Exposed	Unexposed
1	6	Li*	0.02	1.00	0.15	<b>50</b>	7.5
2	7	Li*	0.02	9.00	0.28	<b>450</b>	14
3	10	B*	0.01	0.01	0.01	<b>1</b>	1
4	11	B*	0.10	7.00	0.01	<b>70</b>	0.1
5	51	V*	0.30	30.00	0.20	<b>100</b>	0.7
6	53	Cr	0.60	96.00	1.00	<b>160</b>	1.4
7	54	Fe	2.20	15.00	2.00	<b>6.8</b>	0.9
8	56	Fe	22.20	55.00	20.00	<b>2.5</b>	0.9
9	57	Fe	11.00	45.00	12.00	<b>4.0</b>	1.1
10	60	Ni	0.10	3.00	0.20	<b>30</b>	2
11	61	Ni	0.20	10.00	0.20	<b>50</b>	1.0
12	63	Cu	1.40	60.00	1.00	<b>42.85</b>	0.7
13	87	Sr*	0.10	1.00	0.10	<b>10</b>	1
14	88	Sr*	0.50	0.10	0.20	<b>0.2</b>	0.4
15	90	Zr*	0.01	57.00	0.01	<b>5700</b>	1
16	91	Zr*	0.10	34.00	0.10	<b>340</b>	1

The observed increase in content of chemical elements in: Li by factor of 50–450, <sup>11</sup>B by a factor of 70, Zr by a factor of ~5700, V by a factor of 100, Cr by a factor of 160, Fe by a factor of 2–7, and Ni by a factor of 5–30.

1. The analyzed layer depth ~ 100.

2. Li, B, V, Sr, and Zr were not present in the GD chamber earlier.

3.\*The source of possible impurity is absent.

were published in previous papers [1,2]. Neutrons with energies up to 17 MeV were detected. We also observed an anomalous intensity ratio ranging 2.45 MeV/14 MeV in the neutron groups. This is an evidence of an anomalous type of nuclear reaction [1,2]. The Post-experimental blackening of X-ray films in contact with Pd, Ti, and Ag foils was observed [3–6].

Uranium radioactivity change was also observed after the exposure to D and H GD [7–9]. Post-experimental increase (by four times) in alpha emissions was registered in D discharge after 500 h exposure (for the exposed and unexposed sides). The increase in beta and gamma emissions intensity showed no more than 60% as compared to alpha emissions. The comparison of energy peaks intensity in the gamma spectra evidences that the isotopic ratio intensity (counts per second is cps) of thorium and uranium in energy peaks was changed [10]. Post-experimental changes in uranium alpha, beta and gamma emissions were detected for both sides of the 0.2 mm thick uranium (irradiated and back side) [10,11].

This paper contains a short review of transmutation results in gas GD cathode materials and the accompanying processes [13]. The paper describes isotopic and elemental changes, the associated gamma emissions. The possible mechanism is proposed.

The article presents post-experimental registration lighter isotopes in tungsten and tantalum foils (after the exposure to deuterium GD) using X-ray/gamma spectrometry. Two series of experiments with W foils are described in this review. The first set includes the results of Thermal Ionization Mass Spectrometry (TIMS) analysis, which started ~80

**Table 2.** Dose versus additional atoms quantity upon Pd surface after exposure to Deuterium GD (EDA) [6]

No.	The additional atoms	Atom number	Dependence of additional atoms quantity on dose $\times 10^{-2}$ at.%	
			4 h	40 h
1	Na	11	$7.0 \pm 0.3$	$3.0 \pm 0.3$
2	Mg	12	$1.0 \pm 0.3$	$2.0 \pm 0.3$
3	Al	13	$4.0 \pm 0.3$	$2.0 \pm 0.3$
4	Si**	14	$1.5 \pm 0.3$	$< 0.3$
5	Ca	20	$4.0 \pm 0.3$	$3.0 \pm 0.3$
6	Ti*	22	$1.0 \pm 0.3$	$1.5 \pm 0.3$
7	Br*	35	$3.0 \pm 0.6$	$2.0 \pm 0.6$
8	Sr*	38	$7.0 \pm 0.6$	$6.0 \pm 0.6$
9	Y*	39	$40.0 \pm 1.0$	$20.0 \pm 1.0$
10	Mo**	42	$15.0 \pm 1.0$	$40.0 \pm 1.0$
11	Tc*	43	$20.0 \pm 1.0$	$10.0 \pm 1.0$

EDA is SEM “HITACHI-800” with “Link Analytical” device. Probe diameter of analyzed place was  $\sim 1 \mu\text{m}$ .

\*Source of impurity is absent.

\*\*Sources of possible impurity are the parts of the of discharge chamber.

min after the GD current switch off (there was a 15-minute interval between each analysis). The second set of results included W foils analysis after 3–5 months after the experiment.

## 2. Methods

### 2.1. Experimental method

Deuterium discharge was experimental method of low-energy nuclear reaction initiated. The experimental setup is shown in Fig. 1.

The glow discharge apparatus was made with double quartz tubes (as the wall of the discharge chamber) with cooling water between these quartz tubes. The anode and cathode were cooled with flowing water also. The sequence of operations before discharge experiments was as follows: vacuum degassing to  $10^{-3}$  Torr, followed by deuterium loading to between 3 and 10 Torr. Molybdenum was used as the anode. The used foil was placed on the cathode. The foil  $\sim 100 \mu\text{m}$  thick and  $\sim 20$  mm in diameter. The installation had a vacuum discharge chamber with a cathode and an anode. Deuterium, hydrogen, argon, xenon were used as working gases. Samples were irradiated with gas ion current density of  $10\text{--}200 \text{ mA/cm}^2$  and with discharge voltage of  $50\text{--}1200$  V. The discharge burning exposure was  $1\text{--}40$  h, diameter of the used foils  $\sim 20$  mm, thickness  $\sim 100 \mu\text{m}$ , the irradiated area about  $1 \text{ cm}^2$ .

### 2.2. Methods of the analysis

The examinations procedure in detail is described in [3,4]. The analytical methods included: secondary ions mass spectrometry (SIMS), secondary ions mass spectrometry with additional ionization of the neutral pattering particles (SNMS), spark mass-spectrometry (SMS), thomoionization mass spectrometry (TIMS), energy dispersive analyses (EDA) and high resolution gamma-spectrometry. Changes in the element composition were analyzed with EDA methods and the isotope composition was analyzed with mass spectrometry. The elemental composition of the cathode

materials was studied on scanning electronic microscope Hitachi S-840 with Link Analytical LS-5 and JEOL JSM 6460-LV using INCA for X-ray spectral analysis.

The analyzed zone size was about  $1\ \mu\text{m}^2$  for the probe analysis in point, and up to  $\sim 250 \times 200\ \mu\text{m}^2$  the scanning area. Sensitivity of the method was  $\sim 10^{-2}$  atom.%. Depth of an analyzed layer about 1 mk was used. Concentration of the impurity (“additional”) elements was determined using the majority of main lines of the characteristic X-ray spectrum. Initial samples and samples after experiments in gas glow discharge are analyzed. Places with structural defects and new formations such as swellings (blisters), craters, areas of micromeltings, needle structures, and sites of surface without special changes after and before irradiation in glow discharge plasma were explored.

### 2.2.1. Characterization of TIMS analysis

The isotope composition of the foils at high temperature was determined with TIMS using mass-spectrometers “Finnigan”-262 and Thermo Finnigan “Triton”. The most detailed analyses were performed in the range of mass numbers 166–206. The temperature between Re ionizer and analyzed foils was  $\sim 1800^\circ\text{C}$  [1–4]. The majority of complex compounds should break up (dissociate) at such a temperature while the secondary ionic mass spectrometry can give many composite complexes. The analyzed tungsten strip had the width  $\sim 1$  mm, the length  $\sim 20$  mm and the thickness  $\sim 100\ \mu\text{m}$ . The strip was cut off from the central part of W or Ta foils, irradiated by deuterons. The analyzed zone included the unirradiated part of W foil as well as irradiated parts, which led to a reduced contribution by more light isotopes. The spectra of minimal intensity (CPS) were removed from the table of TIMS data. The data regarding to mass numbers 185 and 187 corresponding to rhenium (Re) isotopes were removed from the table data as well, because Re was used as mass-spectrometer cathode. Two W foils layers were placed on the cathode of gas discharge device. The side of the foil irradiated with deuterium ions was analyzed.

## 3. Results

The analysis of metal foils after the exposure to GD low-energy ions by SIMS, TIMS, SNMS has shown sharp deviations in isotopic ratio ranging 2–10 times, changes in the elemental content (impurity yield increase, occurrence of additional elements), structural changes (formation of new structures, traces of micro-explosions, melting, occurrence of “hot points”), excess heat production, change in gamma-, alpha- and beta-emissions, neutron bursts [1–13].

### 3.1. Dependence of “Additional” elements quantity upon ions type

The dependence of quantity and variation in different additional elements in Pd foils after the exposure to Deuterium, Hydrogen and Ar + Xe was established [5]. It was shown, that the maximum quantity of additional elements occurs after the exposure in Deuterium GD. The ratio may be presented as D: H: (Ar + Xe) = 10: (2–3):1, correspondingly [5].

### 3.2. Dependence of “Additional” elements quantity upon in the ion dose, current type, place and method of analysis.

#### 3.2.1. Dependence of “Additional” elements quantity upon the ion dose, and method of analysis

All the characteristic spectra peaks of Ti, Br, Sr, Y, and Tc were observed. Ti, Br, Sr, Y, and Tc were no observed in the discharge chamber before the exposure. The decrease in Na, Mg, and Ca after the 40-hour experiment with EDA method can be explained by participation of these elements in secondary transmutations or by lighter elements sputtering.

**Table 3.** “Additional” atoms quantity versus ions dose upon Pd surface after exposure to deuterium GD (SMS) [6].

Mass	Element	Before $\times 10^{-4}$ at.%, ( $\times 100$ ppm)	Additional element in Pd for different ex- posure time $\times 10^{-4}$ at. %				Mass	Element	Before, $10^{-4}$ at. % $\times 100$ ppm	$\times$ Additional element content in Pd for different ex- perimental time $\times 10^{-4}$ at. %			
			4 h		40 h					4 h		40 h	
			Upper	Lower	Upper	Lower				Upper	Lower	Upper	Lower
6	Li	0.06	0.15	0	0	0	49	Ti*	1.30	680.00	3.25	28	115
7	Li	0.06	<b>0.33</b>	<b>0.40</b>	0.90	0.50	50	Ti*	1.70	0	3.40	130.0	
10	B	0.07	0	0.15	0	0	78	Se*	0.23	0.23	0.20	0.20	4.00
11	B	0.07	<b>0.30</b>	<b>0.20</b>	0.20	0.70	80	Se*	0.30	0.20	0.20	0.20	33.00
23	Na	0.44	<b>4.40</b>	<b>1.00</b>	2.00	6.00	85	Rb*	< 0.03	0.01	0.05	90.00	51.00
27	Al	6.00	96.00	10.00	300.0	25.00	90	Zr*	< 0.05	25.00	0.05	60.00	0.22
28	Si**	9.00	18.00	9.00	0	3.00	91	Zr*	< 0.05	50.00	< 0.05	61.00	0
29	Si**	7.00	21.00	11.00	0	10.00	93	Nb*	< 2.00	40.00	2.00	7200	4.00
30	Si**	6.00	18.00	4.50	15.00	66.00	98	Mo**	0.40	0	0	0	3.00
32	S	7.00	14.00	2.00	3.50	2.00	100	Mo**	1.80	4500.0	1.80	2880	0
39	K	3.00	9.00	0	12.00	4.50	103	Rh*	7.00	21.00	21.00	25.00	7.00
41	K	3.00	12.00	1.00	18.00	9.00	107	Ag*	<b>1.00</b>	<b>63.00</b>	<b>3.00</b>	<b>1.00</b>	3.20
47	Ti*	1.20	1.80	60.00	0	0	109	Ag*	<b>1.00</b>	<b>50.00</b>	<b>1.50</b>	0	2.50
48	Ti*	1.40	580.0	2.50	0	3.50	115	In*	< 0.04	<b>0.48</b>	<b>0.04</b>	<b>0.80</b>	<b>0.16</b>

**Table 4.** Change of Ag quantity in Pd glow-discharge cathode at various ions density (SMS) [7].

No.	Current (mA)	Type of ions	Analyzed layer *	Ag+2 (ppm)		The factor of increasing (after/initial)
				Isotope mass		
				107	109	
Initial	0		1	17	22	
1666	35	D	1	5000	5200	~ 250
			2	2100	2200	~ 100
			3	<	<	-
				15	5	
1667	35	H	1	110	77	~ 4
			2	<	<	-
				20	20	
			3	<	<	-
1668	25	H/D		20	20	
			1	570	560	~ 25
			2	690	740	~ 35
			3	120	130	~ 5
1670	25	H	1	1000	1000	~ 50
			2	450	450	~ 20
1671	25	D	1	2600	2700	~ 120
			2	1800	1900	~ 9.0

1, 2, 3 are the first, the second and the third analyzed 10  $\mu\text{m}$ -thick layers.

1 is the first upper 10  $\mu\text{m}$ -thick layer of exposed side of the Pd foil.

2 is the second (next) 10  $\mu\text{m}$ -thick layer of exposed side of the Pd foil.

3 is the first layer of the back unexposed side of the Pd foil.

The analyzed layer depth was  $\sim 10 \mu\text{m}$ . Sensitivity of the method was  $\sim 10^{-6}$  at.%.  $^{80}\text{Se}$  content increases by  $\sim 100$  times. 1000-fold increase in Zr and 3000-fold increase in Rb content is shown. Ag content increased by 50 times.  $^{11}\text{B}$  increased by a factor of 10; In increased by a factor 10–20.

### 3.2.2. Ag content in post-experimental Pd versus kind of ions

The maximum Ag content increase in the near-surface layer is 5–100 times bigger in deuterium GD than in hydrogen GD for the same current density.

### 3.2.3. “Additional” elements quantity in Pd versus type of current

The increase in isotopes with lighter masses is more noticeable. The light isotopes sputtering can change the isotopic ratio by percents, but the isotopic ratio change that we observed amounted to  $\sim 10$ –100 times. A considerable increase in  $^{57}\text{Fe}$  content is also observed.

**Table 5.** Isotopic and elemental composition in Pd after the exposure to direct current Deuterium GD (TIMS) [2]

Mass	Element	Natural (%)	CPS1 1610/1	CPS2 1610/2	CPS1–CPS2	Mass	Element	Natural(%)	CPS1 1610/1	CPS2 1610/2	CPS1–CPS2
14	N	90.6	–	–		45	Sc	100	$1.2 \times 10^3$	95	$+1.1 \times 10^3$
15		0.37	20	–	+ 20	46	Ti	8.0	50	65	–15
16	O	99.8	–	–		47		7.3	30	55	–25
18		0.20	10	–	+10	48		73.8	$1.2 \times 10^2$	$4 \times 10^2$	$-2.8 \times 10^2$
22	Ne	9.32	60	10	+ 50	49		5.5	10	45	–35
24	Mg	78.99	10	38	– 28	50	Ti, Cr	5.4, 4.3	$4.6 \times 10^2$	$2 \times 10^2$	$+2.6 \times 10^2$
25		10	–	10	– 10	51	V	99.8	$4.6 \times 10^2$	$5 \times 10^2$	– 40
26		11	–	–		52	Cr	83.8	$1 \times 10^4$	$3.4 \times 10^3$	$+6.6 \times 10^3$
27	Al	100	$1 \times 10^3$	$1 \times 10^4$	$+9 \times 10^3$	53		9.5	$7 \times 10^2$	$3 \times 10^2$	$+4 \times 10^2$
28	Si	92.23	$2.5 \times 10^2$	10	$+2.4 \times 10^2$	54	Fe, Cr	5.8; 2.37	$2 \times 10^3$	$2.6 \times 10^2$	$+1.74 \times 10^3$
29		4.68	–	$1.5 \times 10^2$	$-1.5 \times 10^2$	55	Mn	100	$4 \times 10^3$	30	$+3.97 \times 10^3$
30		3.09	–	30	– 30	56	Fe	91.7	$1.5 \times 10^4$	$2.5 \times 10^3$	$+1.25 \times 10^4$
42	Ca	0.65	$1.8 \times 10^3$	$1.5 \times 10^2$	$+1.65 \times 10^3$	57		2.2	$1.5 \times 10^3$	55	$+1.45 \times 10^3$
43		0.14	$4.3 \times 10^3$	$1.5 \times 10^2$	$+4.15 \times 10^3$	58		0.28	$3.8 \times 10^2$	30	$+3.5 \times 10^2$
44		2.09	10	$6 \times 10^2$	$-5.9 \times 10^2$	59	Co	100	$3.8 \times 10^2$	20	$+3.6 \times 10^2$

1610 (1) is exposed Pd foil; 1610, (2) shows screened Pd foil located under the exposed one (both are 100  $\mu\text{m}$ -thick). There is no reason for the formation of Sc, Cr, Co, and Fe in the upper Pd foil facing the GD. It is suggested that the formation of Sc, Co, and Mn, the increase in Fe, Cr, and Al content in upper Pd foil results from the transmutation. It should be noted that the presence of masses with numbers 22, 45, 55 and 59 in the post-experimental Pd exposed to D GD is observed almost in all the experiments (CPS-count per second).

**Table 6.** Change in Fe, Cr, and Ti isotopic ratio in Pd exposed to direct current GD by TIMS in cps [2].

Mass	Element	Natural abundance (%)	Before CPS	After (CPS*)	exper.	Isotopic ratio, natural ( $N_n$ )	Isotopic ratio after experiment ( $N_{\text{after}}$ )	$N_n / N_{\text{after}}$	CPS ratio after/ before
24	Mg	78.99	8	$50/8 \times 10^{2*}$		24/25–8	24/25–12	$\sim 7 \times 10^{-1}$	6–100
25		10	8	0/67		25/26–1	25/26–1/0.5*	$2 \times 10^0$	0–8
26		11	8	0/38		24/26–8	24/26–1/0.5*	$1.6 \times 10^1$	0–5
28	Si	92.23	8	$1 \times 10^2 / > 1 \times 10^{2*}$		28/29–20	28/29–0.16	$1.25 \times 10^2$	$\sim 12$
29		4.67	8	$6.3 \times 10^2 / 1 \times 10^{3*}$					<b>78–125</b>
30		3.1	8	$2.2 \times 10^2 / 5 \times 10^{2*}$		28/30–30	28/30–0.5	$\sim 6 \times 10^1$	<b>27–62</b>
40	Ca	96.86	8	$1 \times 10^6$		40/44–50	40/44–5	$\sim 1 \cdot 10^1$	$\sim 1 \times 10^5$
42		<b>0.6</b>	<b><math>3 \times 10^3</math></b>	<b><math>2 \times 10^5</math></b>		<b>44/42–3</b>	<b><math>44/42-2.5 \times 10^2</math></b>	<b><math>8 \times 10^1</math></b>	<b><math>\sim 67</math></b>
43		0.15	$2 \times 10^2$	$\sim 4 \times 10^3$		44/42 $\sim 13.3$	44/42– 1.25	$\sim 1 \times 10^{-1}$	<b>20</b>
44		2.0	$1 \times 10^3$	$\sim 5 \times 10^3$					<b>5</b>
45	Sc	<b>100</b>	<b>8</b>	<b><math>2 \times 10^2</math></b>		–	–	–	<b>25</b>
46	Ti	8	65	$1.3 \times 10^3$		48/46–6.2	48/46–5.46	$\sim 9 \times 10^{-1}$	<b>20</b>
47		7.3	95	0					0
48		73.8	$1 \times 10^3$	$7 \times 10^3$					7
56	Fe	91.7	$2.8 \times 10^3$	$4.5 \times 10^3$		56/57–41.7	56/57–18	$\sim 2.3 \times 10^0$	$\sim 1.6$
57		2.2	50	$2.5 \times 10^2$					5
59	Co	100	8	$1.5 \times 10^3$		–	–	–	$\sim 187$

\*x/y stands for the measured spectrum (first spectrum CPS /2-nd spectrum CPS).  $N_n/N_{\text{after}}$  is the isotopic ratio change.



**Table 7.** The isotopic ratio change in “additional” elements in Pd exposed to pulsed-current GD (TIMS) [2].

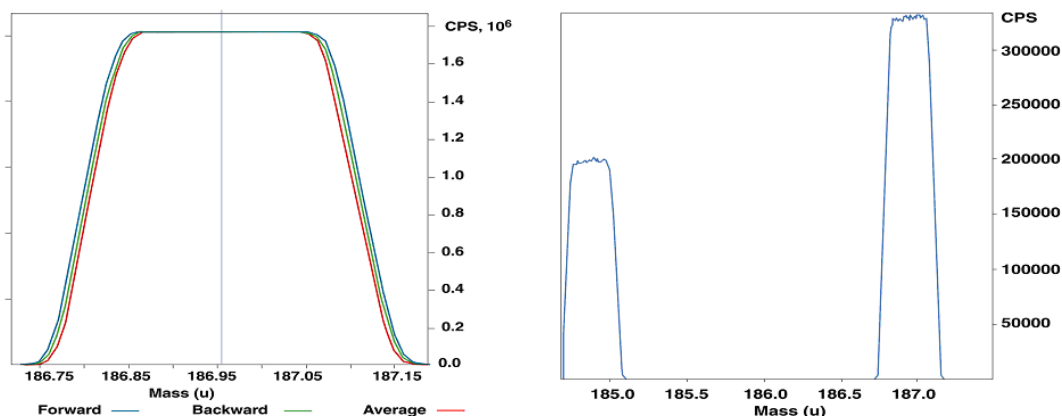
Element	Isotopic ratio	Natural isotopic ratio ( $N_n$ )	Ratio after experiment ( $N_{after}$ )	$N_n / N_{after}$
Si	28/29	93.2/4.7 = 22.6	10/75 = 0.13	$1.73 \times 10^2$
	28/30	93.2/3.1 = 29.8	10/20 = 0.5	$5.96 \times 10^1$
Ne	20/21	90.5/0.27 = 33.5	20/30 = 0.67	$5.0 \times 10^1$
	20/22	90.5/9.3 = 29.7	20/50 = 0.4	$7 \times 4 \cdot 10^1$
Ni	58/60	68.1/26.2 = 2.6	$1.5 \times 10^2 / 6.5 \cdot 10^2 = 0.23$	$1.1 \times 10^1$
	58/61	68.1/1.25 = 55	$1.5 \times 10^2 / 3 \times 10^1 = 5$	$1.1 \times 10^1$
	58/62	68.1/3.6 = 19	$1.5 \times 10^2 / 1.3 \times 10^2 = 1.15$	$1.65 \times 10^1$
Fe	56/57	91.2/2.2 = 41.45	$1.6 \times 10^2 / 4 \times 10^3 = 0.04$	$1.036 \times 10^3$
Cr	52/53	83.8/9.5 = 8.82	$4.8 \times 10^2 / 4.5 \times 10^2 = 1.066$	8. 26
Ti	48/47	73.8/8 = ~9	$2 \times 10^2 / 10 = 20$	0. 5
Ba	138/137	71.7/11.3 = 6.35	$3 \times 10^3 / 1.9 \times 10^2 = 15.8$	0. 4
	138/136	71.7/7.85 = 9.13	$3 \times 10^3 / 120 = 25$	0.36
	138/135	71.7/6.6 = 10.8	$3 \times 10^3 / 2.2 \times 10^2 = 13.63$	<b>0.80</b>
	138/134	71.7/2.4 = $29.8 \times 10^3$	$3 \times 10^3 / 2.5 \times 10^2 = 12$	<b>2.5</b>
Pb	208/207	52.3/22.6 = 2.31	$1 \times 10^2 / 48 = 2.0$	<b>1.1</b>
	208/206	52.3/23.6 = 2.22	$1 \times 10^2 / 40 = 2.5$	<b>0.9</b>

The isotopic deviation after the exposure to direct-current GD amounted to 10–100 times. While the isotopic content of  $^{57}\text{Fe}$  after the exposure to pulsed-current GD increased by 1000.

### 3.3. Post-experimental “Hot” Spots

It is very important to note that the “hot” spots appeared after the exposure to D and H glow discharge:

- The segregations points of Zn, Co, Br, and Mg, were observed mostly on the boundary and sub-boundary of grains with density  $\sim (1-10) \cdot 10^6 \text{ cm}^{-2}$ . Segregation points of Zn  $\sim (1-2) \cdot 10^6 \text{ cm}^{-2}$  and Br  $\sim (2-4) \cdot 10^6 \text{ cm}^{-2}$  on the surface of Pd were registered with the help of microprobe EDX method [6].
- Partial local blackening of X-ray films was observed in places of contact with Pd, Ti, and Ag foils after the exposure in Deuterium GD [6].

**Figure 2.** Calibration of TIMS spectra on isotopes of Rhenium (a).

- Local blackening occurred in X-ray films placed both inside and outside the GD chamber stainless steel wall [6].
- The results of radiography analysis of X-ray films in contact with Pd cathode radioactive isotopes showed the availability of low-energy and high-energy component [6].
- The majority of “additional” elements, formed after the exposure to GD, were found in local zones (hot spots) [1,2].
- The observed effects were explained by a fusion–fission reaction on the cathode; as a result of interaction between the palladium crystal lattice with Deuterium and by the subsequent decay into lighter elements.

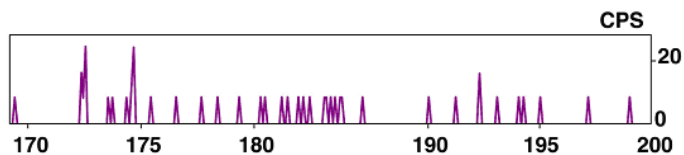


**Figure 3.** Mass spectra of original W in the 170-200 range of masses (CPS).

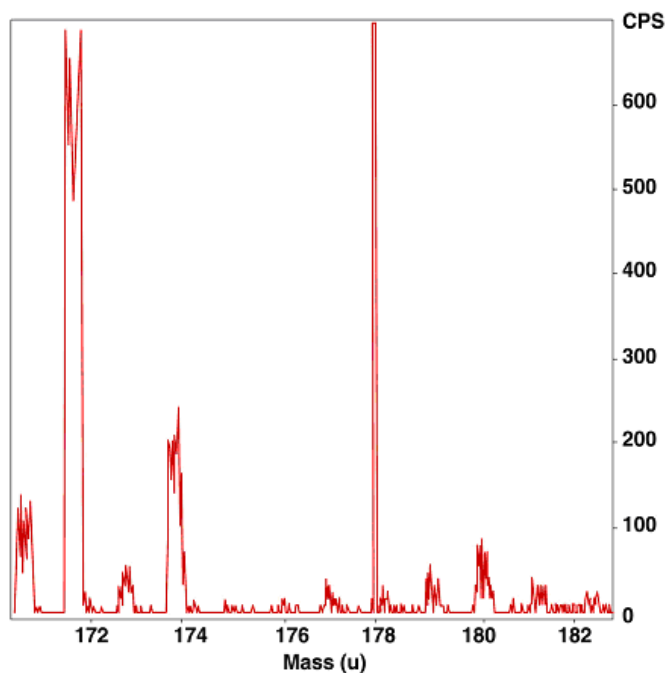


**Figure 4.** Tungsten mass spectra after deuterium discharge for the same foils (Mass: 172–700 cps).

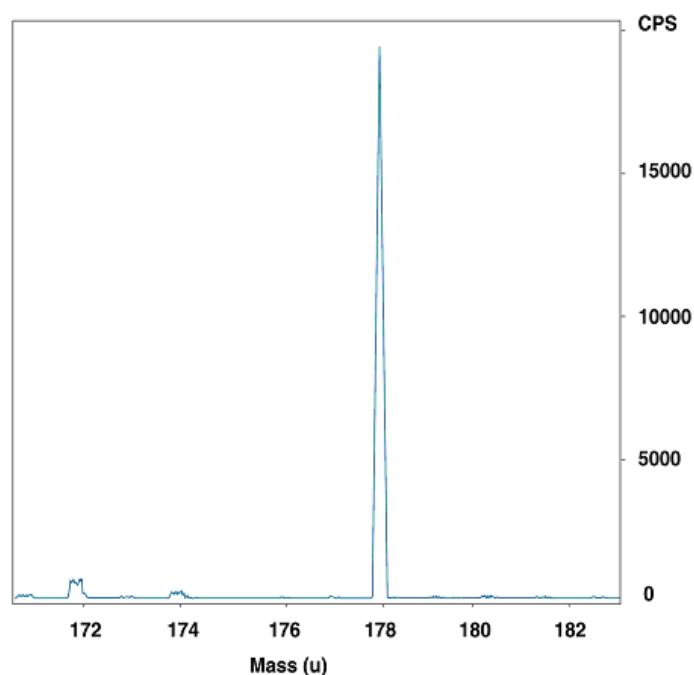


**Figure 5.** Tungsten mass spectra after deuterium discharge for the same foils (Mass: 178–20 000 cps).

### 3.4. Correlation of mass-spectrometry data with X-ray and gamma-emission [3,4]

Possible isotopes correlating to energy peaks in gamma/X-ray spectra were determined and compared to isotopic mass peaks intensity in mass-spectra.

Isotopes of lighter elements during and after the exposure in D GD were selected based upon the block of energy peaks for each isotope (Table of Radioactive isotopes) and upon the mass spectrometry data.

#### 3.4.1. The change of isotopic composition in W after GD with TIMS [3]

Figures 2 and 3 show the calibration of TIMS spectra upon the Rhenium cathode. TIMS spectra measurements have good reproducibility. It can be seen for calibration spectrum on Re, performed before each investigation of new foil. The good reproducibility remained for short time intervals between scanned spectra practically always. An example of a precise definition of isotope mass is shown in the left spectrum, where we can see that 186.95 mass is  $^{187}\text{Re}$  estimated very exactly. Peaks of  $^{185}\text{Re}$  and of  $^{187}\text{Re}$  isotopes are presented in the spectrum on the right.

The significant difference in isotopes intensity was found for the different conditions of experiments: especially, for dose of exposure and time interval after the experiment stopped. The spectra reproducibility is confirmed on the mass-spectra, observed through short time-interval, for example, through  $\sim 3$  min. It was possible to estimate that the intensity of main isotopes is closed for the both spectra. The main isotopes and their intensity are proportional to each other.

As noted above, two series of experiments with W and Ta samples were performed: 15 min after irradiation

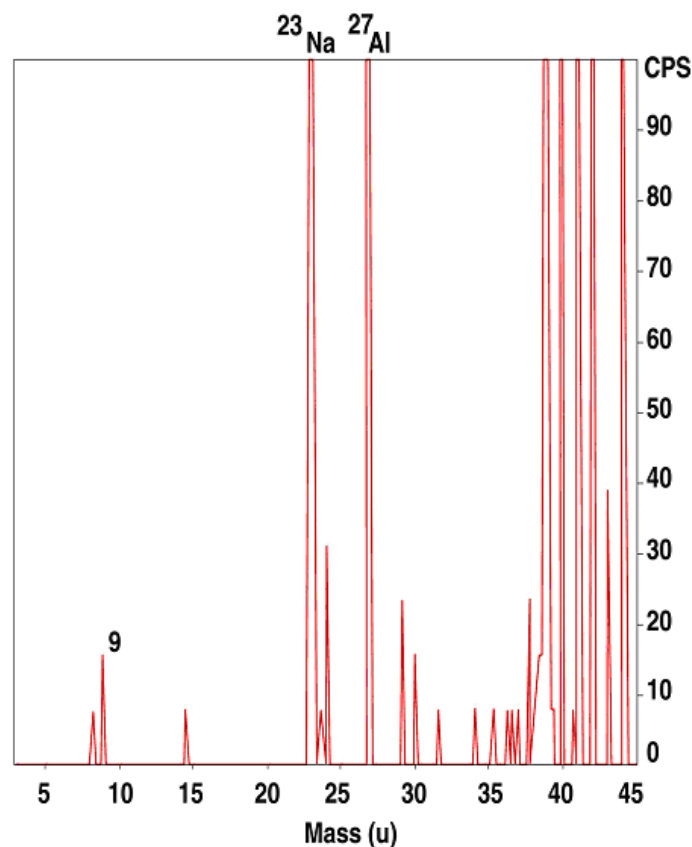


**Figure 6.** The intensity increasing of mass 9 in Ta after deuterium discharge (a).

(Table 8), and 3, 4 and 5 months after experiments (Table 9) both using TIMS.

Tables 8 and 9 compare mass spectra data from the original W and W after deuterium bombardment. The main isotopes changes in the different experiments with W and Ta foils for various time intervals were investigated in detail for the mass range 166–210. An increase in isotopes with masses lighter than tungsten by factors ranging from 5 to 400 was found. The analysis temperature was  $\sim 1800^\circ\text{C}$ . A mass spectrum in original W with 170–200 masses range shown in Fig. 4 the intensity of the separate isotopes from 10 to 30 cps.

A mass spectrum of the W after deuterium discharge for the mass region 170–182 for the same foil with two-minute intervals is shown in Figs. 5 and 6. Mass 172 is  $\sim 700$  cps on the left spectrum, and mass 178 is  $\sim 20\,000$  cps on the right spectrum. The intensity of these isotopes was 10–50 cps before experiments for similar scanning parameters. The increase of masses 172 and 178 intensity in the same tungsten foil was from 12 to 400 times, respectively.

The same result with increasing light mass 171 was observed for tantalum foil. The intensity of mass 171 was  $\sim 50$  cps before the experiment, and after the experiment it reached 19 500 cps, increasing by a factor of  $\sim 390$ . Ta has only single stable isotope  $^{181}\text{Ta}$ .

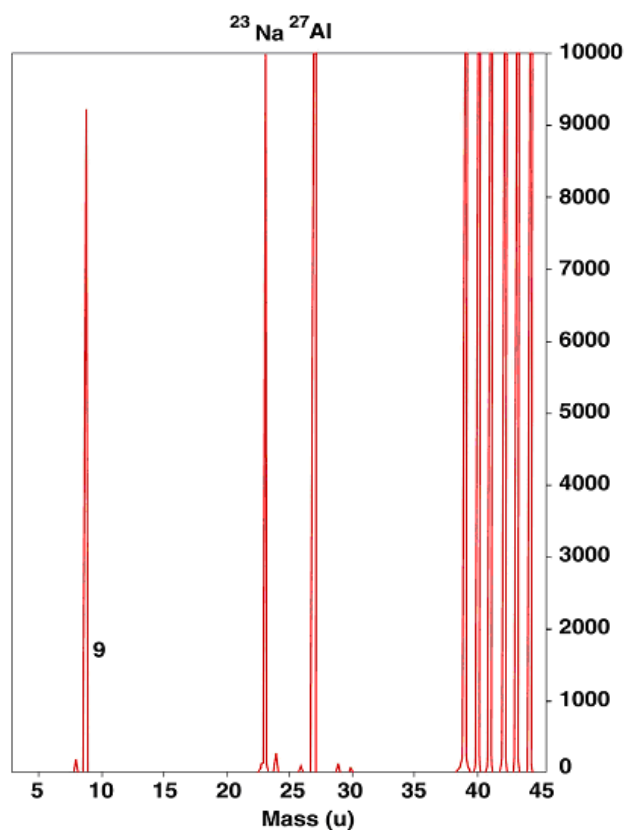


**Figure 7.** The intensity increasing of mass 9 in Ta after deuterium discharge (b).

Figures 7 and 8 show mass 9 in Ta before and after of the deuterium discharge. Mass 9 increased from 20 cps in original Ta foil to 9500 cps in post-experimental foil. The increase was a factor of  $\sim 475$ .

Table 8 shows data from the first set of the experiments with W, showing that transmutation of heavier isotopes into lighter ones continues after the experiment is stopped. Increases from  $\sim 20$  to  $\sim 200$  times for different isotopes were found.

An analysis of tungsten foils irradiated with different doses of deuterium discharge performed 3, 4, and 5 months after irradiation is presented in Table 9.

The lighter masses appearance was observed after GD. Mass spectroscopy results include the following:

- Tungsten transmutation of heavy isotopes into lighter isotopes after exposure in deuterium discharge was confirmed.
- The group of lighter isotopes with mass numbers 169, 170, 171, 178, and 180 had high intensity after deuterium discharge soon after the experiment, and 3, 4, and 5 months later.
- Isotopes with lighter masses (in compare to W isotopes) continued forming for at least 3–5 months after the exposure in the deuterium discharge. The observed increase of different light isotopes was into 5–400 times

(from 5 to 50 cps in the original W into 100–20 000 cps after experiments).

- Experiment with tantalum was carried out to strengthen understanding of the possible reaction. Tantalum was

**Table 8.** Intensity of more light isotopes in tungsten foils after deuterium discharge with TIMS analysis in CPS (set 1)

Time (min*)	84*	101*	137*	1062*	1073*	1133*	1150*	**0, Original W
Mass								
168			40	30	60	2000	30	10 ± 10
170			40	55	50	1600	100	5 ± 5
171			60	95	100	100	70	5 ± 5
172			70	100	100	200	100	0
173			80	75	70	300	100	15 ± 15
174			30	55	60	200	100	5 ± 5
175			40	55	70	40	85	5 ± 5
176			40	55	40	95	75	5 ± 5
177			40	55	40	10	100	10 ± 10
180		70	10	45	100	20	30	25 ± 5
181		100	10	30	40	50		5 ± 5
189	70		20	30	10		50	5 ± 5
193	60		20	30	10		0	5 ± 5
194	70		40	65	0		10	10 ± 10

\* First line shows the time in minutes after experiment.

\*\* Last column is intensity of isotopes in the original W.

\*\*\* Set 1- The first analysis was carried out in 45 min after experiment stop. Farther the each analysis was fulfilled every 15 min during ~3 h and then analysis was made in ~10 h every 15 min during few hours.

**Table 9.** Intensity of isotopes with masses lighter than tungsten isotopes foils after deuterium GD, analyzed with TIMS ( counts per second (CPS) Set No. 2)

No.	No. 1817				No. 1820					No. 1821	Original
Date Mass	16.03*	16.03*	19.03*	20.03*	21.04**	21.04**	23.04**	14.05***	14.05***	20.03***	****
1	2	3	4	5	6	7	8	9	10	11	12
168		0			235	200	75		130		30 ± 10
169		25			475	500	85		243		30 ± 10
170		70			600	600			243		30 ± 10
171	40	70	40	45	950	950	150	140	1670	25	35 ± 10
172	80	80	55	55	5000	6000	700	15	40	65	20 ± 10
173	400	400	300	300	200	200	50	40	488	200	25 ± 10
174	45	50	25	30	1600	1615	230	8	0	46	15 ± 10
175	125	170	75	80	15		15	35	300	70	20 ± 5
176*	8	8	8	8	30		15	50	0		20 ± 5
177	8	8	8	0	30		40	130	35		8 ± 1
178	15	8	0	8	50		19500	20	30		8 ± 1
179	0	8	0	8	70		60	220	100		30 ± 10
180	25	15	8	0			80	480	320		20 ± 5
181			0	120			40	1000			30±5

\*2–5, 11 present the date later tree months after experiments; \*\*6–8 present the date later 4 months after experiments; \*\*\*9–10 present the date later 5 months after experiments; 12\*\*\*\* is average CPS for 3–5 original analyzed foils.

**Table 10.** Tungsten and tantalum energy peaks after deuterium glow discharge in contact with X-ray/gamma CdTe detector (for the one group of isotopes) [4].

W	W	W	Ta	Isotope	$E_\gamma$ (keV)	Half-life	Decay mode	$I_\gamma$ (%)	Mass according TIMS spectra
(1-4) 1817	1820	1818	1824						
Peaks energy of gamma spectra (keV)									
	20.7	20.7	20.7 ± 1	$^{170}_{72}\text{Yb}$	20.75	32d	$\varepsilon$	0.19	169
42 ± 1	43	42	42.18	$^{170}_{72}\text{Yb}$	42.76	32d	$\varepsilon$	0.25	169
50 ± 1	51.2	50.44	51	$^{170}_{72}\text{Yb}$	51.1	32d	$\varepsilon$	0.018	169
63 ± 1	63	62.83	63.5 ± 0.5	$^{170}_{72}\text{Yb}$	63.12	32d	$\varepsilon$	44.2	169
45 ± 1	45.10	44.46	46.46	$^{170}_{72}\text{Hf}$	44.52	16.01 h	$\varepsilon + \beta^+$	0.32	170
55.4	55.5	55.4	55.4	$^{170}_{72}\text{Hf}$	55.2	16.01 h	$\varepsilon + \beta^+$	1.1	170
99.9	99.0	100.8	100.8	$^{170}_{72}\text{Hf}$	99.93	16.01 h	$\varepsilon + \beta^+$	2	170
113.2	113.3	113.2	113.2	$^{170}_{72}\text{Hf}$	113.9	16.01 h	$\varepsilon + \beta^+$	0.18	170
115.6	115.0	115.7	115.6	$^{170}_{72}\text{Hf}$	115.5	16.01 h	$\varepsilon + \beta^+$	0.2	170
133.0	132.0	132.2	132.7	$^{170}_{72}\text{Hf}$	132.2	16.01 h	$\varepsilon + \beta^+$	0.044	170
138.81	138.5	138.0	138.8	$^{170}_{72}\text{Hf}$	139.2	16.01 h	$\varepsilon + \beta^+$	0.018	170
19 ± 1	19.89	19.06	19.1	$^{171m}_{72}\text{Yb}$	19.39	5.25 ms	IT	14.8	171
22.5 ± 1	23.19	23.19	23.2	$^{172}_{72}\text{Hf}$	23.4	1.87 y	$\varepsilon$		172
24 ± 1	24	24.02	24.84	$^{172}_{72}\text{Hf}$	23.93	1.87 y	$\varepsilon$	20.3	172
60 ± 1	60.5	60.35	60.5 ± 0.5	$^{172}_{72}\text{Hf}$	60.65	1.87 y	$\varepsilon$	1.1	172
67 ± 1	63	62.35	67.5	$^{172}_{72}\text{Hf}$	67.3	1.87 y	$\varepsilon$	5.3	172
91 ± 1	91 ± 1	91.74	91	$^{172}_{72}\text{Hf}$	91.3	1.87 y	$\varepsilon$	0.11	172
115 ± 1	114	114.03	114.03	$^{172}_{72}\text{Hf}$	114.06	1.87 y	$\varepsilon$	2.6	172
115 ± 1		115	115.6	$^{172}_{72}\text{Hf}$	116.1	1.87 y	$\varepsilon$	0.034	172
119 ± 1	119	118.99	119.8	$^{172}_{72}\text{Hf}$	119	1.87 y	$\varepsilon$		172
129.03	129	127.25	127.5	$^{172}_{72}\text{Hf}$	127.9	1.87 y	$\varepsilon$	1.46	172
42 ± 1	43	42	42.18	$^{178}_{70}\text{Yb}$	42.4	74 m	$\beta^-$	6.7	178
13 ± 1	14.1	14.1	13.3	$^{180}_{70}\text{Yb}$	13.9	2.4 m	$\beta^-$		180
57 ± 1	58.7	57.05	57.88	$^{180m}_{72}\text{Hf}$	57.555	<b>5.5h</b>	IT	48.0	180m

selected because it has only one stable isotope, with mass number 181.

### 3.4.2. Observation of some isotopes in W after GD with CdTe gamma and X-ray detector [4]

Average intensity of gamma-emission with CdTe gamma and X-ray detector in usual configuration of glow discharge apparatus and original W as background was  $\sim 0.10$  cps.

Calibration of CdTe detector was fulfilled according  $^{133}\text{Ba}$ .

The presents of  $K_a$  series and  $K_b$  series lines of W (in energy regions 57, 58, 59 and 67–69 keV) is evidence of the reality of the identified with using series of pear energy on the observed gamma and X-ray spectra.

Masses in right coulomb were found with a thermal ionization mass spectrometer. It is possible  $^{180m}_{72}\text{Hf}$  nine energy peaks of gamma-spectra correspond with  $^{172}_{72}\text{Hf}$  isotope and seven  $^{172}_{72}\text{Hf}$  peaks of gamma-spectra correspond with

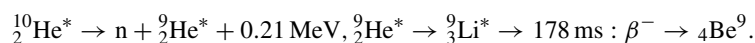
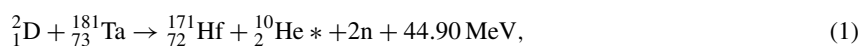
$^{170}_{72}\text{Hf}$   $^{180\text{m}}_{72}\text{Hf}$  isotope. The isotope  $^{180\text{m}}_{72}\text{Hf}$  with IT 99.7%.  $\beta$ - 0.3% and  $T_{1/2} = 5.47$  h was assumed taking into account the maximal intensity of gamma-emission in 5.5 h time exposure.

The correlation of gamma and X-ray emission with mass-spectrometry data allows to have of opinion that the process of formation new isotopes are going during and after glow discharge [3,4].

Some variants of the way for isotope transformation under glow discharge was suggested early [1,4].

#### 4. Discussion

Only one possible example of reaction taking into account the masses defect, spin and parity estimation is suggested below:



There are also alternative assumptions which may provide a better explanation of the details of this complex process, for example the poly-neutron theory of transmutation, suggested by John Fisher [15] or the stimulation of LENR by the electro-magnetic excitation of the crystal lattice in [5,9] and by Peter Hagelstein [16].

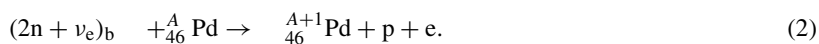
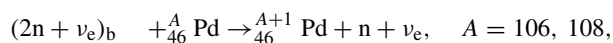
Presently, there are more than 150 theories and assumptions to explain low-energy nuclear reactions, some of them suggested by Russian researchers: the flux hypothesis by Boris Rodionov [17] based on the existence of cylindrical atoms, the idea of Vladimir Muromtsev about the cluster decay and neutrino–dineutron reactions, based on the neutrino interaction with elements and the resulting dineutrons formation [18], and the Unitary Quantum theory by Lev Sapogin [19].

The latest explanation of LENR phenomena in terms of classic nuclear physics was suggested by Ratis [20]. This explanation involves the reaction of nuclei-target with dineutroneum atoms, which represent a bound state of two neutrons and one neutrino generated by the inclusive electronic capture (EC) reaction  $e^- + d \rightarrow (2n + \nu_e)_b + X$ .

Ratis [20] suggests that the dineutroneum atoms are metastable particles with the life-time of  $(2n + \nu_e)_b \sim 3 \times 10^{-3} \text{ s}$ , by three orders more than the  $\mu$ - meson life-time. The size of the dineutroneum atom is commensurable with the size of the deuteron. The mass of the dineutroneum atom is equal to  $M_{(2n+\nu_e)_b} = 2.014102236 \text{ e}^- = 1876.0965 \text{ MeV}$ .

The metastability, electrical neutrality and the small sizes of the dineutroneum atoms allows them to take part in the fusion reaction with nuclei-targets.

In the deuterium plasma (in GD) may takes places generation of the dineutroneum atoms  $(2n + \nu_e)_b$  (b- bound). These atoms collides with  $^{106}_{46}\text{Pd}$  and  $^{108}_{46}\text{Pd}$  nuclei in the Pd-cathode in the discharge chamber. As a result, one can observe reactions



Formula (2) gives us an answer to a question, why neutrons are registered so rarely in CF reactions. Neutrino is a very light particle, and palladium is a very heavy particle. In the neutron transfer reaction the  $(n + \nu_e)_f$  –the rest does not practically interact with the Pd-nucleus. As a rule, the only open channel of the compound particle  $(n + \nu_e)_f$  decay – the rest is  $p + e^-$ . We cannot observe a free neutron and neutrino in the exit channel of the  $(n + \nu_e)_f$  -decay reaction,



because it is forbidden by conservation law (neutrino has a very large energy, and a very small momentum). Thus, the channel  $(n + \nu_e)$  is closed. In contrast to the previous case, all particles in the  $p+e^-$  - channel have an electrical charge. Both particles – proton and electron – interact with a Pd-nucleus. The mass of electron is by many orders more than the mass of neutrino, and it carries away not only energy, but also momentum. As a result, the  $p+e^-$  channel of the  $(n+e^-)_f$  -decay opens up [20].

## 5. Conclusion

- (1) The presence of low-energy nuclear reactions was confirmed by the GD low-energy influence:
  - Significant increase in additional elements ranging 10 -1000 times was found.
  - Isotopic deviation in materials (Pd, Ti, W, and U) and the increase in the additional impurity elements from 2 up to 100 times was discovered.
  - The majority of the newly formed elements, found after the GD switch off were found in certain local zones (“hot” spots, micro melting points) on the cathode material surface.
  - Post-experimental isotopes with masses of 169, 170, 171, 178, and 181 (less than W and Ta isotopes) were found with the help of TIMS.
  - The isotopic changes continue to occur for at least 3–5 months after the GD exposure. Separate isotopes with masses less than W and Ta isotopes have grown by factors ranging 5–1000 times.
  - The same energy peaks in gamma-spectra occur during and after the GD current switch-off.
  - The change in alpha, beta, gamma radioactivity caused by the GD was observed.
  - Post experimental weak gamma, X-ray and beta- emissions were detected.
- (2) The correlation between the gamma and X-ray emission data and the thermal ionization mass-spectrometry data for the same isotopes is shown in the W foils.  
 The comparison of the mass spectra and the gamma spectra points to the existence of the following isotopes:  
 $^{169}\text{Yb}$ ;  $^{170}\text{Hf}$ ;  $^{171m}\text{Yb}$ ;  $^{172}\text{Hf}$ ;  $^{178}\text{Yb}$ .
- (3) The collection of effects confirms availability of nuclear transformations under exposure to GD low-energy ions bombardment in materials and in other processes.
- (4) The GD low-energy influence can be used in new power engineering and new technologies (e.g., isotope production). The described effects should be paid more attention to.

## References

- [1] I. Savvatimova and D. Gavritenkov, Results of analysis of Ti foil after glow discharge, *Proc. ICCF11*, World Scientific, France, 2004, pp. 438–458.
- [2] I. Savvatimova and D. Gavritenkov, Influence of the glow discharge parameters on the structure and isotope composition of cathode materials, *Proc. ICCF12, 2005*, World Scientific, Japan, pp. 231–252.
- [3] I. Savvatimova, Creation of more light elements in tungsten irradiated by low-energy deuterium ions, *ICCF13*, Russia, 2008, pp. 505–517.
- [4] I. Savvatimova, G. Savvatimov and A. Kornilova, Decay in tungsten irradiated by low energy deuterium ions, *ICCF13*, Russia, 2008, pp. 295–308.
- [5] I. Savvatimova, A. Senchukov and I. Chernov, Transmutation phenomena in the palladium cathode after ions irradiation at glow discharge. proceedings, *ICCF6*, Japan, 1996, pp. 575–579.
- [6] I. Savvatimova, Ya Kuchero and A. Karabut, Cathode material change after deuterium glow discharge experiments, *ICCF4*, Dec. 1993, *Trans. Fusion Technol.* **26** (4T) (1994) 389–394.
- [7] I.B. Savvatimova and A.B. Karabut, Nuclear Reaction Products Registration on the Cathode after Deuterium Glow Discharge, *Surface*, V. 1, Moscow: RAN, 1996, pp. 63–75.

- [8] I. Savvatimova, Transmutation in cathode materials exposed at glow discharge by low energy ions, Nuclear phenomena or ion irradiation result? *Proc. ICCF-7*, Canada, Vancouver, 1998, pp. 342–350.
- [9] A.B. Karabut, Ya.R. Kuchеров and I.B. Savvatimova, Nuclear product ratio for glow discharge in deuterium, *Phys. Lett. A* **170** (1992) 265–272.
- [10] A.B. Karabut, Ya.R. Kuchеров and I.B. Savvatimova, The investigation of deuterium nuclei fusion at glow discharge cathode, *Fusion Technol.* **20** (1991) 924–928.
- [11] I.B. Savvatimova, Reproducibility of experimental in glow discharge and process accompanying deuterium ions bombardment, *ICCF8*, Italian Phys. Soc, Italy, 2000, p. 277.
- [12] J. Dash, I. Savvatimova, S. Frantz, E. Weis and H. Kozima, Effects of glow discharge with hydrogen isotope plasmas on radioactivity, *Proc. ICENES*, 2002, p. 122.
- [13] J. Dash, I. Savvatimova, S. Frantz, *Proc. 11th Int. Conf. on Emerging Nuclear Energy Systems*, Univ New Mexico, Albuquerque, NM, 2002, pp. 122–127.
- [14] J. Dash and I. Savvatimova, Effects of glow discharge with hydrogen isotope plasmas on radioactivity of uranium, *Proc. American Nucl. Soc. Conf.*, San Diego, 6 June, 2003.
- [15] J. Fisher, Polynutron theory of transmutation, *Proc. 12 Int. Conf. on Cold Fusion ICCF12*, Yokohama, Japan, 2005, pp. 516–520.
- [16] P. Hagelstein, *Proc. 6th Int. Conf. on Cold Fusion ICCF6*, Oct. 13–18, 1996, Japan, 1996.
- [17] B. Rodionov and I. Savvatimova, Unusual structures on the material surfaces irradiated by low energy ions, *ICCF12*, Japan, 2005.
- [18] V. Muromtzev, V. Platonov and I. Savvatimova, Neutrino-dineutron reactions, *Proc. the ICCF12*, Yokohama, Japan, 2005, pp. 571–576.
- [19] L. Sapogin, *Unitary Quantum Theory*, Moscow, Russia, 2005.
- [20] Yu. L. Ratis, *Controlled Hot fusion or Cold Fusion? Drama of Ideas*, 2009, Samara, Russia, 102 p.